Materials Research Proceedings 35 (2023) 173-181 https://doi.org/10.21741/9781644902714-21

Reverse bending fatigue of 316L stainless steel components produced by laser powder bed fusion

Stefano Guarino[1,2,a], Emanuele Mingione[1,2,b], Gennaro Salvatore Ponticelli[1,2,c,*], and Simone Venettacci[1,2,d]

[1]University Niccolò Cusano, Department of Engineering, Via Don Carlo Gnocchi 3, 00166 Rome, Italy

[2]ATHENA European University

[a]stefano.guarino@unicusano.it, [b]emanuele.mingione@unicusano.it, [c]gennaro.ponticelli@unicusano.it, [d]simone.venettacci@unicusano.it

Keywords: Laser Powder Bed Fusion, 316L Stainless Steel, Fatigue Life

Abstract. The freedom to manufacture metal components with very complex geometries using additive manufacturing techniques, such as laser powder bed fusion (LPBF), has opened new possibilities to produce innovative solutions with a high technological impact. It is therefore pivotal to have a detailed knowledge of the performance characteristics, both in the short and in the long term. Within this framework, this study firstly highlights the monotonic tensile properties of the LPBF samples by changing the laser scanning speed, the layer thickness, and the building orientation. Then, within the same process conditions, the fatigue life is investigated through reverse bending loading tests. The results verify an improved resistance, a reduced rigidity, and a strong anisotropy for the LPBF specimens if compared to the bulk material. The dependence on the orientation, together with the porosity of the LPBF samples, are the primarily responsible for the reduction of the fatigue limit.

Introduction

Stainless steels are metallic materials of high mechanical properties, good machinability, excellent corrosion resistance and low production costs. These properties promote their wide application in numerous engineering sectors, from biomedical, to automotive, aerospace, and so forth [1]. However, the traditional processes for producing this alloy, based on the subtraction of material, are characterised by low production flexibility, severe limitations in terms of complexity of the final part, as well as considerable investment costs and high resource consumption. The recent development and industrialisation of innovative non-conventional technologies have made it possible to overcome these barriers, providing more sustainable solutions than traditional processes [2].

Additive Manufacturing (AM) technologies have allowed to eliminate limitations on the complexity of geometry, materials, and level of customization, greatly increasing the process flexibility and prototyping capabilities [3], and, at the same, time reducing manufacturing waste and increasing process automation and sustainability [4]. Laser Powder Bed Fusion (LPBF) represents the most widely used and studied AM technology in industry and research. LPBF processes apply selective fusion of metal powders through the action of a high-power laser beam in an inert chamber, thus generating layer by layer a finished object with excellent mechanical performance and a high level of precision [5]. The current major limitations of LPBF processes are low productivity and high uncertainty regarding the quality and mechanical performance of the produced components [6], mainly due to the presence of defects such as trapped gas, unmelted material, oxides, etc. [7]. Therefore, a detailed knowledge of both the physics and the effect of

Content from this work may be used under the terms of the Creative Commons Attribution 3.0 license. Any further distribution of this work must maintain attribution to the author(s) and the title of the work, journal citation and DOI. Published under license by Materials Research Forum LLC.

Materials Research Proceedings 35 (2023) 173-181 https://doi.org/10.21741/9781644902714-21

process parameters on microstructure, internal defects, and mechanical performance, is necessary to guarantee long-lasting and good reliability in service of the products [8].

In this context, the characterisation of the fatigue life of LPBF-ed 316 L components is a subject worthy of much more in-depth study. This work therefore proposes to first analyse the mechanical and surface properties of the LPBF-ed samples, then to investigate their fatigue performance, by comparing the results with conventional 316L specimens. To this end, tests were first carried out under static tensile loading, then by applying a cyclic loading-unloading force, and finally, by means of reverse bending for fatigue life evaluation.

Experimental

The research study aims at evaluating the mechanical properties of 316L stainless steel components produced by using the laser powder bed fusion technique and compared with traditionally hot rolled laminates cut by laser (named "bulk" in the following). The experimental approach consisted in three main steps: (i) static monotonic tensile tests, to evaluate the fundamental mechanical properties and the initial data set to define the procedure of the following steps; (ii) load-unload tensile cyclic tests; (iii) reverse bending fatigue tests.

Materials and sample preparation

The material adopted to fabricate the samples by LPBF is a commercial metal powder with an average diameter of 32.4 μm supplied by Sandvik Osprey Ltd. and processed with the SLM 280HL machine by SLM Solutions Group. While the bulk samples have been cut starting from a 3 mm thick sheet laminate supplied by Hans-Erich Gemmel & Co. by using the CO_2 laser cutting machine TruLaser Cell 7020 by Trumpf. Table 1 and Table 2 show the main characteristics of the starting materials and the main features of the processing machines, as declared by the suppliers. Table 3 summarizes the design of the experiments based on the main process parameters, i.e. laser power, laser scanning speed, hatch distance, layer thickness, and building orientation. The choice was made according to preliminary studies aimed at obtaining full-dense samples for LPBF and minimizing burr formation for laser cutting. The geometry of the samples was the same for all the tests, according to the standards ASTM E8/E8M and ISO 3928 (Fig. 1).

Table 1 – Main characteristics and chemical composition of the starting materials.

Characteristic	**LPBF**				**Bulk**			
Melting point [°C]	1371-1399				1385-1400			
Density [g/cm^3]	7.87				7.91			
Chemical composition [wt%]	Cr	16.9	P	0.03	Cr	17.5-19.5	P	0.045
	Ni	10.5	C	0.014	Ni	8.5-10.5	C	0.07
	Mo	2.3	S	0.005	Mo	-	S	0.03
	Mn	0.99	N	-	Mn	2	N	0.11
	Si	0.66	Fe	Bal.	Si	1	Fe	Bal.

Table 2 – Machine configurations for LPBF and laser cutting.

Feature	**SLM 280HM**	**TruLaser Cell 7020**
Working volume XYZ [mm^3]	280×280×365	2000x1500x750
Max. laser power [W]	400	4000
Layer thickness [μm]	20-90	-
Laser beam focus diameter [μm]	80-115	50
Max. laser scanning speed [m/s]	10	2.5
Average gas consumption in process [L/min]	2.5 (Ar)	348 (N_2)

Materials Research Proceedings 35 (2023) 173-181 https://doi.org/10.21741/9781644902714-21

Table 3 – Process parameters adopted to produce the samples.

Parameter	LPBF			Bulk
Laser power [W]	175			2800
Hatch distance [µm]	100			-
Laser scanning speed [mm/s]	750			50
Layer thickness [µm]	30			-
Building orientation [°]	0	45	90	-

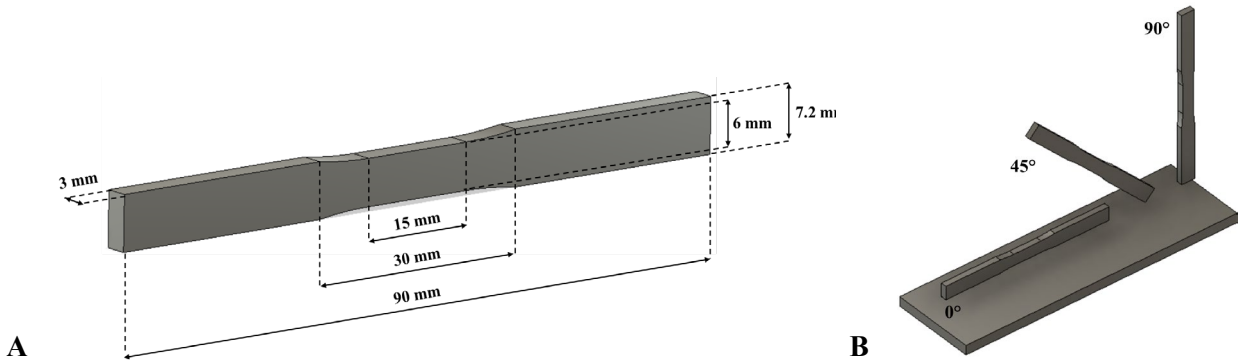

Figure 1 – Schematic representation of A) sample geometry and B) building orientation.

Characterization tests

The study of the mechanical properties was carried out by performing three different tests. At first, the fundamental mechanical properties, as elastic modulus (*E*), yield strength (*Ys*), and ultimate tensile strength (*UTS*) were evaluated through monotonic quasi-static tensile tests by using the 50 kN MTS Insight Electromechanical Testing System with a crosshead speed set at 1.2 mm/min according to the ASTM E8/E8M standard. Then, the load-unload tests were completed on the same machine by applying an increasing load of 500 N every cycle, while the pure reverse bending tests were performed by using the 3 kN MTS Acumen Electrodynamic Testing System with a sinusoidal load and a frequency of 5 Hz. The latter tests were conducted on ad hoc designed bending system, shown in Fig. 2, in which is also schematized the bending moment distribution along the sample surface, being constant and resulting from the vertical load transferred by the top grip. The tests were considered valid over $8 \cdot 10^3$ cycles and marked as run-out after $2 \cdot 10^6$ cycles [9]. It is worth noting that all the tests were carried out at ambient temperature after preparing the samples by wire-cutting and grinding them to remove any unwanted protrusions.

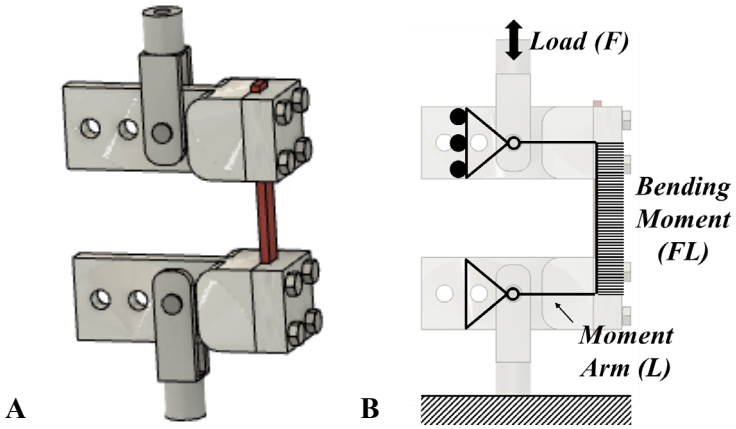

Figure 2 – Schematic representation of A) bending system and B) moment distribution.

After the tests, the failure surfaces were analysed with the scanning electron microscope SEM Leo SUPRA 35 by ZEISS. Moreover, the surface roughness was quantified by means of the

Materials Research Proceedings 35 (2023) 173-181 https://doi.org/10.21741/9781644902714-21

arithmetical mean height of the surface parameter (Sa) according to the standard ISO 25178. The measurements, three for each sample, were performed before testing by using the 3D surface profiling system Talisurf CLI 2000 and further elaborated with the software MountainsMap® 7 by Digital Surf.

Results and Discussion

Quasi-static tensile characterization

The first step of the characterization dealt with the evaluation of the mechanical properties under quasi-static load and the comparison with bulk samples produced through conventional casting process. In this way, it was possible to define the range of loads which will be used during the following fatigue life tests. Moreover, the inspection of the surface quality in terms of *Sa* was performed. The main results for each building orientation are summarised in Table 4.

Table 4 – Mechanical and surface properties of the LPBF fabricated samples.

Property	LPBF			Bulk
	0°	45°	90°	
UTS [MPa]	696 ± 25.3	631 ± 12.9	584 ± 12.4	538 ± 12.0
Ys [MPa]	502 ± 14.2	486 ± 15.9	484 ± 10.1	274 ± 6.5
E [GPa]	168 ± 6.2	165 ± 8.8	167 ± 8.0	190 ± 4.4
Sa [µm]	9.86 ± 0.59	9.49 ± 2.97	8.04 ± 0.44	0.26 ± 0.05

Results from the quasi-static characterization highlight an anisotropic effect on both mechanical and surface properties due to the different building orientations along which the samples were fabricated. From the tensile strength values obtained it is notable that the 0° orientation allows the highest values of *UTS* and *Ys*, while for the modulus *E* the difference is negligible. It is worth to note the variability of the results which is quantified through standard deviation (shown in Table 4 after the plus/minus sign). Those results can be explained because larger and more frequent pores, as well as unmelted particles and inclusions, are more frequent at the border and in between two consecutive layers (Fig. 3), thus acting as stress concentrations and inhibiting the mechanical performances [10]. In fact, the 90° samples have layers orthogonally oriented with respect to the applied tension. Therefore, since they have more layer interfaces, a not favourable load orientation, and being the layer interfaces less cohesive areas, this orientation is characterized by the lowest values of *UTS* and *Ys*.

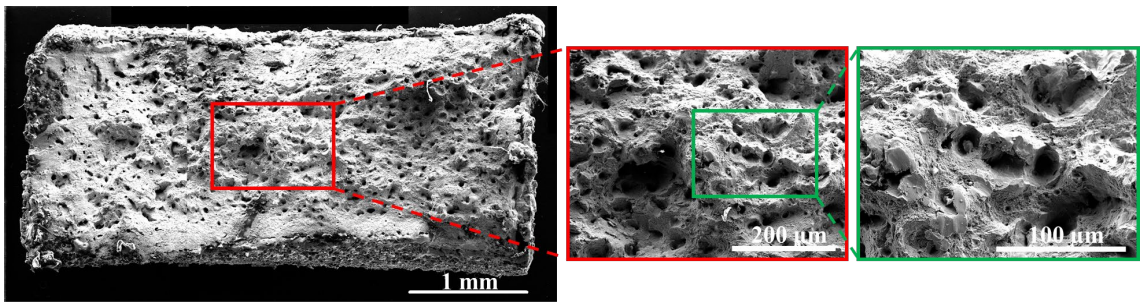

Figure 3 – SEM images of the fracture surface after tensile test of a 45° oriented sample.

It is worth noting that the *Ys* values of the bulk material (274 ±6.5 MPa) are almost the half of those obtained from the 0° oriented samples (502 ±14.2 MPa). Moreover, also *UTS* is improved, as it increases from an average of 538 ± 12.0 MPa of the bulk samples up to 696 ± 25.3 MPa of the horizontal LPBF samples. These results are ascribed to the Hall-Petch phenomena [11], for which the finer the grain size, the higher the number of grain boundaries, the greater the energy needed by a dislocation to move to another grain, and the higher the mechanical strength. In addition, the pile-up of the dislocations near the grain boundaries increases their density and

Materials Research Proceedings 35 (2023) 173-181 https://doi.org/10.21741/9781644902714-21

decreases the free path for their movement [12]. For these reasons, the LPBF samples are more resistant to an external force application.

Despite such improvements, the elastic response of the material changes. The elastic modulus lowers from 190 ±4.4 GPa of the bulk samples down to an average modulus of 169 ±7.5 GPa for the LPBF. According to the literature [13], the reduction of stiffness depends on different factors such as the preferential orientation of the grains along one direction, the presence of porosities into the samples and the higher dislocation density and segregation effect.

The results on *Sa* highlights the most critical aspect of the LPBF process, with values up to 50 times higher. There is not a marked difference between the building orientations since the samples were produced with the same process parameters, however, it can be noted that the standard deviation of the tilted samples is 6 times higher than the others. This can be ascribed to the staircase effect which increase the overall variability of the external surface.

Load-unload tensile characterization

Load-unload tests were performed to evaluate a correlation with the fatigue behaviour of the samples in terms of accumulated damage. The main results of load-unload tests are summarized in Fig. 4, in which are showed the plots for the stress and the displacement (calculated through the extensometer) against time. The tests were carried out in the elastic regime. In fact, despite the increasing load steps at each cycle, the total stress is always lower than the calculated yield strength for each sample. Moreover, the maximum strain is always lower than 0.2% regardless of the experimental condition.

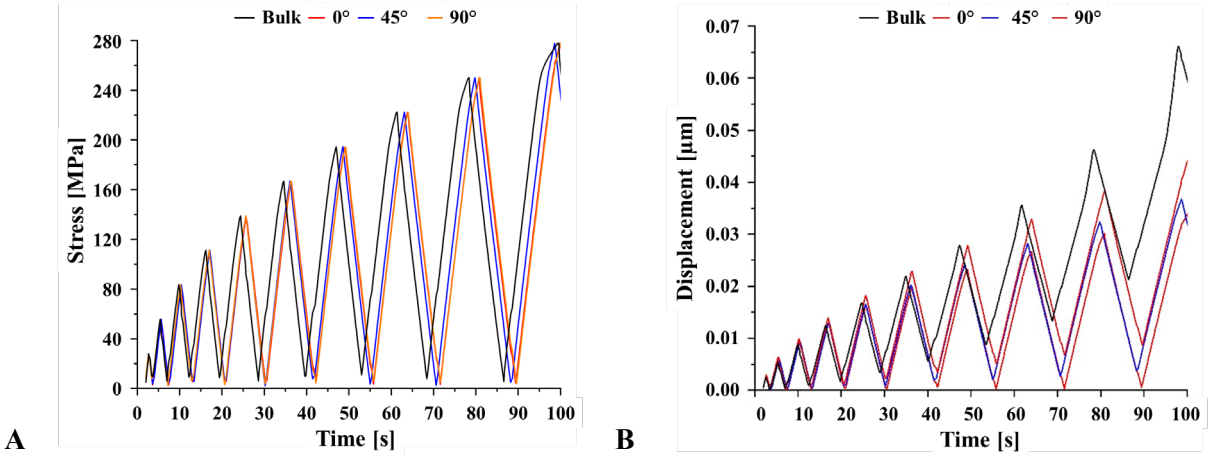

Figure 4 – A) Stress and B) strain over time calculated in load-unload tests.

To evaluate the difference in deformation of the bulk compared to LPBF samples, the maximum and minimum values at each load-unload step were plotted in Fig. 5A. As shown in the latter, the sample with the highest deformation during the loading and unloading phase is the bulk one, followed respectively by the orientations 90°, 45° and 0°. Fig. 5B shows the difference between the maximum and minimum displacement at each cycle, indicated as Δstrain. In particular, a higher value of Δstrain indicates a higher springback of the material. It is worth noting that the bulk is the one with the lowest springback, followed by the LPBF oriented at 90°, 45° and 0°.

Materials Research Proceedings 35 (2023) 173-181 https://doi.org/10.21741/9781644902714-21

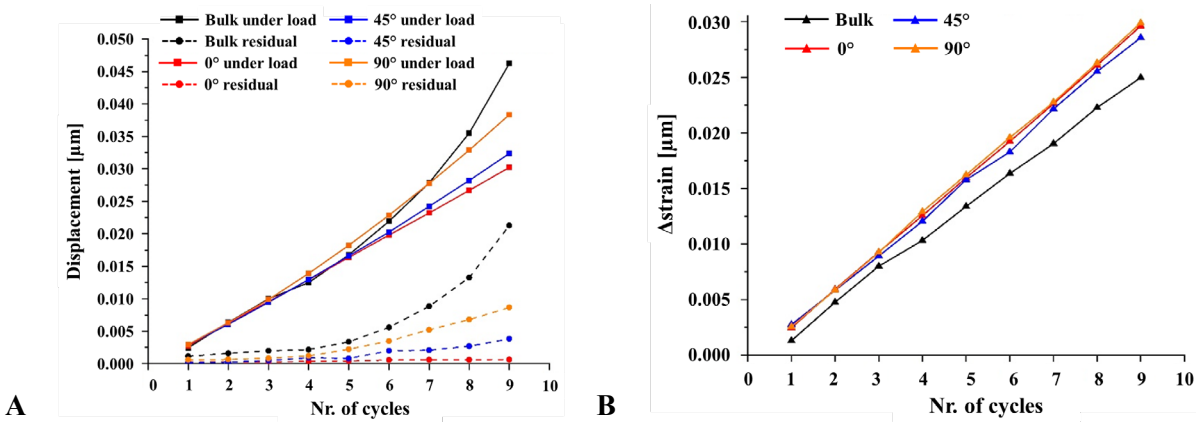

Figure 5 – A) Max. and min. displacement and B) Δstrain induced by load-unload cycles.

However, these results are not indicative to predict the fatigue behaviour since does not consider the damage induced for each cycle. With this aim, the variation of the slopes of the load curves at each cycle were calculated according to Eq. 1, thus, determining the damage induced by the test [14], where E_1 is the elastic modulus at the first cycle, and E_n is the apparent elastic modulus at the n-th cycle. Fig. 6 shows the results.

$$\text{Damage} = (1 - E_n/E_1). \quad (1)$$

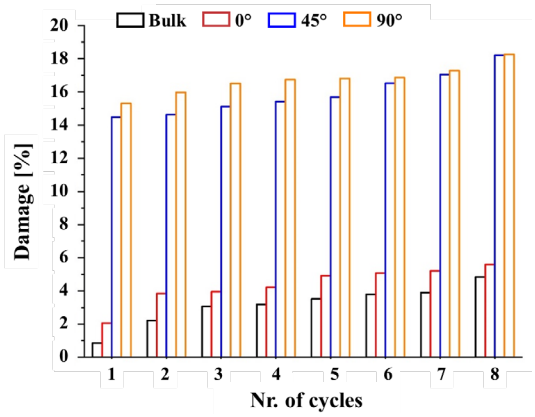

Figure 6 – Damage percentage at each load-unload step.

The LPBF samples with the 90° and 45° orientations present increasingly higher damage values compared to the 0° and the bulk. This result is attributable to the presence of more porosities in the LPBF material, since the most porous zones act as a stress amplifier and a preferential zone in which the crack propagation can start. The difference between the 0° samples compared to the others can be explained since the major porosities and inclusions are present within the printing layers which are oriented in the same direction as the load, as it is for the tilted and vertical samples.

Reverse bending characterization

To confirm the hypothesis from the analysis of the percentage damage, reverse bending fatigue tests were performed. The tests were carried out at varying stress magnitudes spanning the entire finite life region, i.e. from $8 \cdot 10^3$ to $2 \cdot 10^6$ cycles. Based on the previous investigation, the fatigue limit of the specimens is expected to be within the range 0.35 to 0.60 of the tensile strength [15]. To build up the fatigue curves, as a first guess, the reverse bending stress was set equal to around half the ultimate strength from the static tests. The main results are shown in Fig. 7.

Materials Research Proceedings 35 (2023) 173-181 https://doi.org/10.21741/9781644902714-21

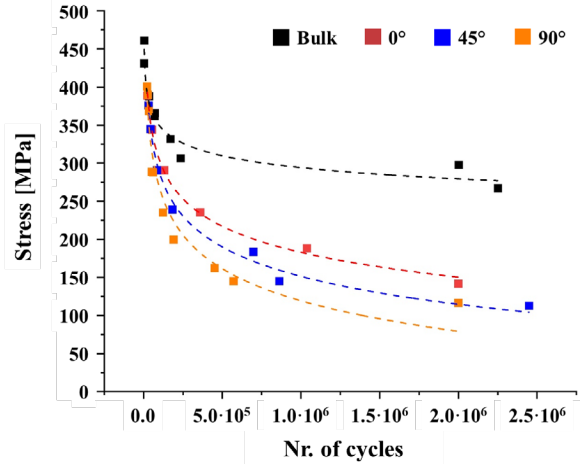

Figure 7 – Fatigue curves comparison.

All the LPBF fabricated specimens have similar low-cycle fatigue responses than the bulk material. This is usually ascribed to high surface roughness, tensile residual stresses, and the presence of pores and other defects that promote crack initiation [16]. The fatigue response of LPBF specimens is further found to be affected by the building orientation. The estimated fatigue limits range from 98.0 MPa for the 90° samples up to 168.3 MPa for 0°, i.e., around 17% and 24% of *UTS*, respectively. The obtained fatigue limits are therefore much lower than the expected fatigue strengths. Moreover, regardless of the parameters' combination, the fatigue strength is less than half of the conventionally processed samples.

The fatigue strength of the horizontal specimens is the highest among the building orientations considered within this study, while the vertical one is characterized by the lowest fatigue limit. This finding is in agreement within the results of the previous damage analysis and can be addressed to the orientation of the deposited layers relative to the applied load, which for the vertical samples is normal to the stress induced by the bending moment. In fact, consecutive layers and their boundaries are characterized by the presence of larger and more frequent pores, as well as unmelted particles and inclusions, therefore, they represent stress concentrators and crack initiators that reduce the fatigue life of the samples [17].

Conclusions

This study investigated the possibility to predict the fatigue behaviour of laser powder bed fused 316L stainless steel samples and traditionally bulk laminates cut by laser, with incremental load-unload tensile cyclic tests. The results obtained were compared with reverse bending fatigue tests on the same samples. The main conclusions which can be drawn are the following:

- During quasi-static tensile tests, the horizontal samples show a doubled yield strength and a 1.3 times ultimate tensile strength than the bulk ones, due to the refining of the grain size through the Hall-Petch phenomena.
- During the incremental load-unload tests, LPBF samples with the 90° and 45° orientations present increasingly higher damage values compared to the 0° and the bulk. This result is attributable to the presence of more porosities within the printing layers in the LPBF material.
- Load-unload tests also confirm the anisotropy highlighted during monotonic tensile tests, showing a worsening trend moving from horizontal to vertical in terms of damage percentage, which increases from approximately 6% up to around 18%.
- The reverse bending fatigue tests confirmed the damage prediction from the incremental load-unload tests since the fatigue behaviour of the horizontal specimens is the best among the building orientations while the vertical one is characterized by the lowest fatigue limit.

References

[1] Shin, W.S.; Son, B.; Song, W.; Sohn, H.; Jang, H.; Kim, Y.J.; Park, C. Heat Treatment Effect on the Microstructure, Mechanical Properties, and Wear Behaviors of Stainless Steel 316L Prepared via Selective Laser Melting. Materials Science and Engineering: A 806 (2021). https://doi.org/10.1016/j.msea.2021.140805

[2] Mehrpouya, M.; Vosooghnia, A.; Dehghanghadikolaei, A.; Fotovvati, B. The Benefits of Additive Manufacturing for Sustainable Design and Production. Sustainable Manufacturing (2021) 29-59. https://doi.org/10.1016/B978-0-12-818115-7.00009-2

[3] Ponticelli, G.S.; Tagliaferri, F.; Venettacci, S.; Horn, M.; Giannini, O.; Guarino, S. Re-Engineering of an Impeller for Submersible Electric Pump to Be Produced by Selective Laser Melting. Applied Sciences (Switzerland) 11 (2021). https://doi.org/10.3390/app11167375

[4] Gardner, L. Metal Additive Manufacturing in Structural Engineering - Review, Advances, Opportunities and Outlook. Structures 47 (2023) 2178-2193. https://doi.org/10.1016/j.istruc.2022.12.039

[5] Yasa, E. Selective Laser Melting: Principles and Surface Quality. Addit Manuf (2021). https://doi.org/10.1016/B978-0-12-818411-0.00017-3

[6] Ponticelli, G.S.; Venettacci, S.; Giannini, O.; Guarino, S.; Horn, M. Fuzzy Process Optimization of Laser Powder Bed Fusion of 316L Stainless Steel. Prog. Addit. Manuf. (2022). https://doi.org/10.1007/s40964-022-00337-z

[7] Liu, Y.; Zhang, M.; Shi, W.; Ma, Y.; Yang, J. Study on Performance Optimization of 316L Stainless Steel Parts by High-Efficiency Selective Laser Melting. Opt Laser Technol 138 (2021). https://doi.org/10.1016/j.optlastec.2020.106872

[8] Blinn, B.; Ley, M.; Buschhorn, N.; Teutsch, R.; Beck, T. Investigation of the Anisotropic Fatigue Behavior of Additively Manufactured Structures Made of AISI 316L with Short-Time Procedures PhyBaL LIT and PhyBaL CHT. Int J Fatigue 124 (2019) 389-399. https://doi.org/10.1016/j.ijfatigue.2019.03.022

[9] Riemer, A.; Leuders, S.; Thöne, M.; Richard, H.A.; Tröster, T.; Niendorf, T. On the Fatigue Crack Growth Behavior in 316L Stainless Steel Manufactured by Selective Laser Melting. Eng Fract Mech 120 (2014) 15-25. https://doi.org/10.1016/j.engfracmech.2014.03.008

[10] Casati, R.; Lemke, J.; Vedani, M. Microstructure and Fracture Behavior of 316L Austenitic Stainless Steel Produced by Selective Laser Melting. J Mater Sci Technol 32 (2016) 738-744. https://doi.org/10.1016/j.jmst.2016.06.016

[11] Tucho, W.M.; Lysne, V.H.; Austbø, H.; Sjolyst-Kverneland, A.; Hansen, V. Investigation of Effects of Process Parameters on Microstructure and Hardness of SLM Manufactured SS316L. J Alloys Compd 740 (2018), 740, 910-925. https://doi.org/10.1016/j.jallcom.2018.01.098

[12] Kocks, U.F.; Mecking, H. Physics and Phenomenology of Strain Hardening: The FCC Case. Prog Mater Sci 48 (2003) 171-273. https://doi.org/10.1016/S0079-6425(02)00003-8

[13] Saeidi, K.; Akhtar, F. Subgrain-Controlled Grain Growth in the Laser-Melted 316 L Promoting Strength at High Temperatures. R Soc Open Sci 5 (2018). https://doi.org/10.1098/rsos.172394

[14] Lemaitre, J.; Desmorat, R. Engineering Damage Mechanics: Ductile, Creep, Fatigue and Brittle Failures; 1st ed.; Springer: Berlin (2005).

[15] ASM International Fatigue. In Elements of Metallurgy and Engineering Alloys; ASM International, Ed.; ASM International: Ohio (2008) 243-264. https://doi.org/10.31399/asm.tb.emea.t52240243

[16] Pellizzari, M.; AlMangour, B.; Benedetti, M.; Furlani, S.; Grzesiak, D.; Deirmina, F. Effects of Building Direction and Defect Sensitivity on the Fatigue Behavior of Additively Manufactured H13 Tool Steel. Theoretical and Applied Fracture Mechanics 108 (2020). https://doi.org/10.1016/j.tafmec.2020.102634

[17] Fotovvati, B.; Namdari, N.; Dehghanghadikolaei, A. Fatigue Performance of Selective Laser Melted Ti6Al4V Components: State of the Art. Mater Res Express 6 (2018). https://doi.org/10.1088/2053-1591/aae10e